Journal of Sound and Vibration 326 (2009) 421–437

Contents lists available at ScienceDirect

Journal of Sound and Vibration

journal homepage: www.elsevier.com/locate/jsvi

Pseudo-inverse Jacobian control with grey relational analysis for robot manipulators mounted on oscillatory bases ☆

J. Lin *, C.C. Lin, H.-S. Lo

Department of Mechanical Engineering, Ching Yun University, 229, Chien-Hsin Road, Jung-Li City, Taiwan 320, ROC

ARTICLE INFO

Article history:
Received 12 October 2008
Received in revised form
20 April 2009
Accepted 25 May 2009
Handling Editor: J. Lam
Available online 21 June 2009

ABSTRACT

Interest in complex robotic systems is growing in new application areas. An example of such a robotic system is a dexterous manipulator mounted on an oscillatory base. In literature, such systems are known as macro/micro systems. This work proposes pseudo-inverse Jacobian feedback control laws and applies grey relational analysis for tuning outer-loop PID control parameters of Cartesian computed-torque control law for robotic manipulators mounted on oscillatory bases. The priority when modifying controller parameters should be the top ranking importance among parameters. Grey relational grade is utilized to investigate the sensitivity of tuning the auxiliary signal PID of the Cartesian computed-torque law to achieve desired performance. Results of this study can be feasible to numerous mechanical systems, such as mobile robots, gantry cranes, underwater robots, and other dynamic systems mounted on oscillatory bases, for moving the end-effector to a desired Cartesian position.

1. Introduction

Complex robotic systems have recently garnered increased attention in many fields. An example of such a system is a dexterous manipulator mounted on a flexible base. In literature, such systems are known as macro-micro systems, characterized by the number of control actuators than state variables [1,2]. In such research, manipulator dynamics are markedly affected by nonlinear forces due to base oscillation and nonlinearity; these include gravity, and Coriolis and centrifugal forces that are typically intrinsic to mechanical systems [3].

Many studies have investigated the flexibly linked elastic-joint robots in terms of joint trajectory control [4], stability of joint-level control [5], and tracking control [1–3,6]. However, maintaining the stability of end-point feedback control with a flexible base remains difficult. If task-space control is applied to flexible-base manipulators without considering base flexibility, a closed-loop system can be destabilized rapidly.

Most work related to oscillatory base manipulators move robots along desired joint angles [1–10]. Controllers for robots described in literature are restricted to tracking joint-space trajectories. However, in practical applications, the desired trajectories of a robotic arm are given in the workspace or as Cartesian coordinates.

In the history of robotics, PD control for not only joint-space control but also task-space control was investigated in [11,12]. Moreover, a task-space PD control does work also for robotic systems with joint redundancy. This means that without compensating the complex nonlinear terms, a task space control works well for position control or stabilization,

☆ Research Supported by National Science Council Research Grant NSC 95-2221-E-231-010.
* Corresponding author. Tel.: +886 3 4581196x3760; fax: +886 3 4598411.
E-mail address: jlin@cyu.edu.tw (J. Lin).

0022-460X/$ - see front matter © 2009 Elsevier Ltd. All rights reserved.
doi:10.1016/j.jsv.2009.05.027

provided PD-gain tuning is accomplished carefully [13–15]. However, none of these studies developed a PD (or PID) controller for the proposed mechanism structure—manipulators mounted on oscillatory bases in task space control.

Exploration on kinematically redundant robots has been flourishing for over two decades, and now is still very active [15]. A manipulator is termed kinematically redundant when it possesses more degrees of freedom than it is needed to execute a given task. Redundancy can be conveniently exploited to achieve more dexterous robot motions. It is widely recognized that a general task consists of following an end-effector motion trajectory is considered as the typical example of intrinsically redundant manipulator. However, even robot arms with fewer degrees of freedom, like conventional six-joint manipulators, may become kinematically redundant for specific tasks, such as simple end-effector positioning without constraints on the orientation. Therefore, the motivation for introducing kinematic redundancy in the mechanical structure of a manipulator goes beyond that for using redundancy in traditional engineering design, explicitly, increasing robustness to faults so as to improve reliability [15].

To move the robotic end-effector to a desired position, knowledge of its kinematics is required to solve an inverse kinematics problem to generate a desired position in the joint space. When the control problem is formulated directly in the task space, the inverse kinematics problem is replaced by the transposed Jacobian matrix, ranging from the joint space to the task space in control law [16]. Ref. [17] described a real-time implementation of a Cartesian-based controller applied to a direct-drive selective compliance assembly robot arm (SCARA) robot with 2 degrees of freedom (dof). This control scheme uses path shapes described in Cartesian coordinates and, therefore, avoids trajectory conversion of joint-based coordinates.

For tasks performed by robotic manipulators, such as moving payloads or painting objects, position controllers give adequate performance as such tasks only require that a robot follows a desired Cartesian trajectory. Therefore, regulating the contact force between the end-effector of the manipulator and the environment is extremely important [18]. Consequently, position/force control must be performed for robot manipulators to achieve such sophisticated tasks.

Many robot-control schemes have been developed. Most can be considered as special cases of computed-torque controllers. The scheme proposed in this study involves decomposition of the control design problem into an inner-loop and outer-loop design problem. Due the simple structure of control type, the proportional-derivative (PD) controller or proportional-integral-derivative (PID) controller has been widely used as the auxiliary control signal for computed-torque controllers [19]. However, the major challenge in producing a satisfactory PID controller is tuning PID controller parameters to achieve desired performance. The method for selecting parameters based on experimental results is usually time-consuming [9,20]. The Ziegler–Nichols ultimate-cycle tuning and closed-loop tuning have been widely accepted as accurate heuristic schemes for determining the appropriate settings for PID and proportional-integral (PI) controllers for numerous industrial applications. However, manual tuning is not often applied in practice because it is laborious and time-consuming, particularly for processes with large time constants. Manual tuning also requires that an instrument/control engineer and operator pay close attention to process, because the process must be operated near instability to measure ultimate gain and period [20].

Grey system theory, pioneered by [21], has been widely applied in numerous fields. Grey theory manages any random data series as a variation in a grey value within a specific range. Recently, grey relational theory has been employed to elucidate the tuning of PID parameters to yield a desired performance. The grey relational decision model, which is one of the most commonly used approaches, is simple, practical and easy to handle [9].

This study presents novel pseudo-inverse Jacobian feedback control laws combined with grey relational analysis for tuning outer-loop PID control parameters of Cartesian computed-torque control laws for robot manipulators mounted on oscillatory bases. This research extends that of [7–9], in which robots move along desired joint angles. Hence, the primary goal in this study is present a novel controller that moves the robotic end-effector to a desired Cartesian position. Experiments are conducted to confirm the efficiency of the proposed methodology. Experimental results demonstrate that the proposed scheme is feasible for developing a controller.

2. System configuration

2.1. Dynamic modeling

Fig. 1 presents the conceptual model of a manipulator mounted on an oscillating base. For convenience, this work considers a special case, a two-link planar arm mounted on an oscillatory base (Fig. 2), with a 2-dof manipulator and 1-dof base motions. The oscillatory dynamics of the base can be simplified as a lumped mass with a spring, and represented as

$$M_b\ddot{x}_b + C_b\dot{x}_b + K_b x_b = f_d, \tag{1}$$

where $x_b \in \Re^p$ denotes the displacement of the base from its equilibrium point. Here, p is defined as the number of dofs of the oscillatory base. Moreover, $M_b \in \Re^{p\times p}$ and $K_b \in \Re^{p\times p}$ are the inertial matrix and stiffness matrix, respectively, and $C_r \in \Re^{p\times p}$ is the damping matrix, and f_d is the excitation force acting on an oscillatory base [1–3].

Additionally, the dynamics of the n rigid-link manipulators with revolutional joints can be expressed as [19]

$$M_r(q)\ddot{q} + C_r(q,\dot{q}) = \tau_r, \tag{2}$$

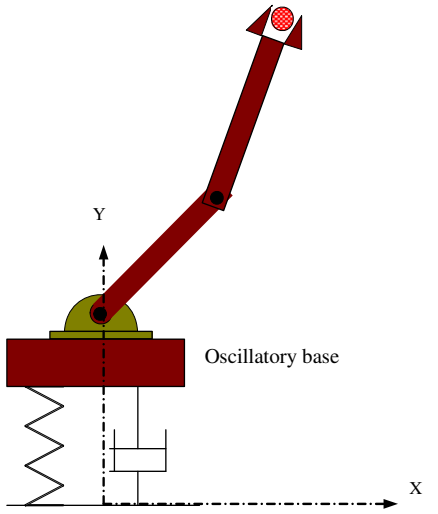

Fig. 1. Conceptual model of compliant manipulators.

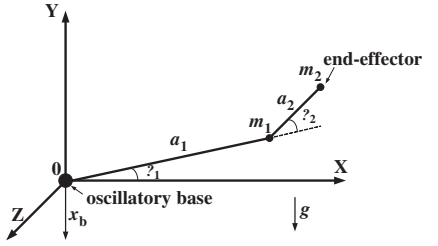

Fig. 2. Schematic view of the manipulator mounted on an oscillatory base.

with $q(t) \in \Re^n$ as the joint variable vector, $M_r \in \Re^{n\times n}$ as the inertia matrix of rigid-link manipulators, and $\tau_r(t) \in \Re^n$ as the control input, where $C_r \in \Re^n$ represents the nonlinear terms, including the Coriolis/centripetal forces, viscous friction, dynamic friction, and gravity.

When the two systems are serially combined, detailed analysis indicates that the overall system can be represented as [7–9]

$$\begin{bmatrix} M_r(q) & M_{br}^{\mathrm{T}}(x) \\ M_{br}(x) & M_b + M_{b/r}(x) \end{bmatrix} \begin{Bmatrix} \ddot{q} \\ \ddot{x}_b \end{Bmatrix} + \begin{bmatrix} C_r(q,\dot{q}) + C_{b/r}(x,\dot{x}) \\ C_b\dot{x}_b + C_{br}(x,\dot{x}) \end{bmatrix} + \begin{bmatrix} 0 & 0 \\ 0 & K_b \end{bmatrix} \begin{Bmatrix} q \\ x_b \end{Bmatrix} = \begin{bmatrix} \tau_1 \\ \tau_2 \end{bmatrix} + \begin{bmatrix} 0 \\ f_d \end{bmatrix}, \tag{3}$$

where $M_{b/r}(x) \in \Re^{p\times p}$ and $M_{br} \in \Re^{p\times n}$ are inertia matrices for the manipulator/base coupling, which is referred to as the inertia coupling matrix; $C_{b/r}(x,\dot{x}) \in \Re^n$ and $C_{br}(x,\dot{x}) \in \Re^p$ are nonlinear coupling terms, and $x = [q \;\; x_b]^{\mathrm{T}} \in \Re^{(n+p)}$. Hence, the overall system dynamics equations can be rewritten as

$$\mathbf{M}(x)\ddot{x} + \mathbf{C}(x,\dot{x}) + \mathbf{K}(x)x = \tau. \tag{4}$$

The inertial matrix of the overall system $\mathbf{M}(x) \in \Re^{(n+p)\times(n+p)}$ shown in Eq. (4) is symmetrical and positive-definite. Therefore, inertial matrix $\mathbf{M}(x)$, which is uniformly bounded from above and below, satisfies

$$\underline{\mathbf{m}} I_{n+p} \le \mathbf{M}(x) \le \overline{\mathbf{m}} I_{n+p}, \quad \forall x \in \Re^{n+p}$$

where $\underline{\mathbf{m}}$ and $\bar{\mathbf{m}}$ are positive constants, and $I_{n+p} \in \Re^{(n+p)\times(n+p)}$ is the identity matrix. By applying Lagrangian formulation, the overall dynamics equation of a two-link planar arm mounted on an oscillatory base is in the same form as that in Eq. (3), where the joint variable is $q = [\theta_1 \;\; \theta_2]^{\mathrm{T}}$, and generalized force vector is $\tau_1 = [u_1 \;\; u_2]^{\mathrm{T}}$, where u_1 and u_2 are joint torques supplied by actuators. Moreover, τ_2 is the control voltage from the force generator that reduces the vibration of the oscillatory bases. For the dynamic derivation procedure, refer to [7–9].

Moreover, the symbolic terms in Eq. (4) are as follows.

$$M_{b/r} = m_1 + m_2,$$

$$M_{br} = \begin{bmatrix} (m_1+m_2)a_1\cos\theta_1 + m_2a_2\cos(\theta_1+\theta_2) & m_2a_2\cos(\theta_1+\theta_2) \end{bmatrix},$$

$$M_r = \begin{bmatrix} (m_1+m_2)a_1^2 + m_2a_2^2 + 2m_2a_1a_2\cos\theta_2 & m_2a_2^2 + m_2a_1a_2\cos\theta_2 \\ m_2a_2^2 + m_2a_1a_2\cos\theta_2 & m_2a_2^2 \end{bmatrix},$$

$$C_{br} = -(m_1+m_2)a_1\dot{\theta}_1^2\sin\theta_1 - m_2a_2(\dot{\theta}_1+\dot{\theta}_2)^2\sin(\theta_1+\theta_2) + (m_1+m_2)gx_b,$$

$$C_r = \begin{bmatrix} -m_2a_1a_2(2\dot{\theta}_1\dot{\theta}_2 + \dot{\theta}_2^2)\sin\theta_2 + (m_1+m_2)ga_1\cos\theta_1 + m_2ga_2\cos(\theta_1+\theta_2) \\ m_2a_1a_2\dot{\theta}_1^2\sin\theta_2 + m_2ga_2\cos(\theta_1+\theta_2) \end{bmatrix},$$

$$C_{b/r} = \begin{bmatrix} -(m_1+m_2)a_1\dot{x}_b\dot{\theta}_1\sin\theta_1 \\ 0 \end{bmatrix},$$

where we assume link masses m_1 and m_2 are concentrated at the ends of the link. Furthermore, a_1 and a_2 are link lengths [7–9].

2.2. Task-space formulation

In most applications, a desired path for the end-effector is specified in a task space such as a Cartesian space. In such a case, the planar arm is mounted on an oscillatory base. Hence, let ϕ be a task space defined as follows:

$$H = \phi(x), \tag{5}$$

where $m \le n+p$ and $\phi : \Re^{(n+p)\times m} \to \Re^m$ is generally a nonlinear transformation describing the relationship between joint space and task space. Here, m defined as the number of degrees of freedom required for the end-effector task. In such a case, this study considers nonredundant robots, where $m = n+p$, and redundant robots, where $m < n+p$. Typically, the joints can provide at least number of degrees of freedom required for the end-effector task.

Task-space velocity $\dot{H}$ is related to joint-space velocity $\dot{x}$ as

$$\dot{H} = J(x)\dot{x} \tag{6}$$

where $J(\cdot) \in \Re^{m\times(n+p)}$ is the Jacobian matrix from the joint space to task space. The above equation is called the first-order differential kinematics.

By differentiating Eq. (6), the Cartesian acceleration term is

$$\ddot{H} = J(x)\ddot{x} + \dot{J}\dot{x} \tag{7}$$

This equation is also known as the second-order differential kinematics.

Moreover, the equation for robot system motion in the joint space can then be represented as Cartesian space coordinates based on the following relationship:

$$\ddot{x} = J(x)^{-1}(\ddot{H} - \dot{J}\dot{x}). \tag{8}$$

Substituting Eq. (8) into Eq. (4) yields

$$\mathbf{M}(x)J(x)^{-1}(\ddot{H} - \dot{J}\dot{x}) + \mathbf{C}(x,\dot{x}) + \mathbf{K}(x)x = \tau \tag{9}$$

where $\mathbf{M}(x) \in \Re^{(n+p)\times(n+p)}$ is total system inertia matrix, $\mathbf{C}(x,\dot{x}) \in \Re^{(n+p)}$ is nonlinear Coriolis/centrifugal terms, and $\mathbf{K}(x) \in \Re^{(n+p)\times(n+p)}$ is stiffness matrix.

The manipulator is nonredundant and, thus, $m = n+p$; however, if it is not the case, the manipulator can be considered as locally redundant. However, in the case of $m < n+p$, additional constraints must be imposed on available joint torques to satisfy the static assumption [16].

To analyze redundant robots ($m < n+p$), the singular value decomposition (SVD) is introduced [15,22]. The SVD of J is given by

$$J = U\Sigma V^{\mathrm{T}} = U\begin{bmatrix} \boldsymbol{\lambda} & O \\ O & O \end{bmatrix}V^{\mathrm{T}} \tag{10}$$

where $U \in \Re^{m\times m}$, $\Sigma \in \Re^{m\times(n+p)}$, $V \in \Re^{(n+p)\times(n+p)}$, and $\boldsymbol{\lambda} = \mathbf{diag}(\lambda_1,\lambda_2,\ldots,\lambda_r)$.

Under the assumption that the manipulator is kinematically redundant (i.e. $m<n+p$), the pseudo-inverse J^+ of J is a matrix that must satisfy

$$\begin{aligned} JJ^+J &= J \\ J^+JJ^+ &= J^+ \\ (JJ^+)^T &= JJ^+ \\ (J^+J)^T &= J^+J \end{aligned} \tag{11}$$

Therefore, the SVD of such a matrix can be written as

$$J^+ = V\begin{bmatrix} \lambda^{-1} & O \\ O & O \end{bmatrix}U^{\mathrm{T}}. \tag{12}$$

If J^+ is low-rectangular and full rank, its pseudo-inverse can be computed as

$$J^+ = J^{\mathrm{T}}(JJ^{\mathrm{T}})^{-1}, \tag{13}$$

and $JJ^+ = I_{(n+p)\times(n+p)}$.

Hence, the dynamic Eq. (9) can be rewritten as

$$\mathbf{M}(x)J^+(x)(\ddot{H} - \dot{J}\dot{x}) + \mathbf{C}(x,\dot{x}) + \mathbf{K}(x)x = \tau. \tag{14}$$

However, in most work, oscillatory base manipulators are designed to move robots along desired joint angles [1–10]. In this section, the output of interest is Cartesian error

$$e_H(t) = H_d(t) - H(t), \tag{15}$$

where $H_d(t)$ is the desired Cartesian trajectory, and $H(t)$ is the end-effector Cartesian position. To determine the influence of input $u(t)$ on tracking error, Eq. (15) is differentiated twice to obtain

$$\begin{aligned} \dot{e}_H(t) &= \dot{H}_d(t) - \dot{H}(t) \\ \ddot{e}_H(t) &= \ddot{H}_d(t) - \ddot{H}(t). \end{aligned} \tag{16}$$

The control input law is defined as

$$\ddot{e}_H(t) = \tau_H. \tag{17}$$

In classical control theory, in the presence of disturbances, PD control generates a nonzero steady-state error [19]. However, at a steady state, a residual error exists due to disturbance and gravity. This error can be removed using the PID computed-torque controller

$$\begin{aligned} \dot{\varepsilon}_H &= e_H(t) \\ \tau_H &= -K_d\dot{e}_H - K_pe_H - K_i\varepsilon_H, \end{aligned} \tag{18}$$

which yields robot manipulator control input

$$\begin{aligned} \tau = \mathbf{M}(x)J^+(x)(\ddot{H}_d - \dot{J}\dot{x} + K_d\dot{e}_H + K_pe_H + K_i\varepsilon_H) \\ + \mathbf{C}(x,\dot{x}) + \mathbf{K}(x)x. \end{aligned} \tag{19}$$

Eq. (19) is called as the "Cartesian computed-torque control law (CCTC)".

However, the control law (19) cannot usually be implemented due to its complexity or to uncertainties present in $\mathbf{M}(x)$, $\mathbf{C}(x,\dot{x})$, and $\mathbf{K}(x)$. Instead, one applies τ in (20) below where $\hat{M}_J(x)$, $\hat{C}(x,\dot{x})$, and $\hat{K}(x)$ are approximations to $\mathbf{M}(x)J^+(x)$, $\mathbf{C}(x,\dot{x})$, and $\mathbf{K}(x)$, respectively,

$$\tau = \hat{M}_J(x)(\ddot{H}_d - \dot{J}\dot{x} + K_d\dot{e}_H + K_pe_H + K_i\varepsilon_H) + \hat{C}(x,\dot{x}) + \hat{K}(x)x. \tag{20}$$

We call Eq. (20) the "approximate Cartesian computed-torque controller (ACCTC)".

In some case $\mathbf{M}(x)$, $\mathbf{C}(x,\dot{x})$, or $\mathbf{K}(x)$ is not known exactly. Then, $\hat{M}_J(x)$, $\hat{C}(x,\dot{x})$, and $\hat{K}(x)$ could be the best estimate we have for these terms. Fundamentally, the Eq. (19) is based on the calculation of the inertia matrix $\mathbf{M}(x)$, Coriolis and centrifugal terms $\mathbf{C}(x,\dot{x})$ and stiffness $\mathbf{K}(x)$. In fact, even if the matrix $\hat{M}_J(x)\neq\mathbf{M}(\mathbf{x})J^+(x)$, $\hat{C}(x,\dot{x})\neq\mathbf{C}(x,\dot{x})$, and $\hat{K}(x)\neq\mathbf{K}(x)$, the performance of controllers based on Eq. (20) can be quite good if the outer-loop gains are selected appropriately [19].

From the projection operator, Eq. (19), (20) can be divided into two control loops—one is the damping controller that suppresses vibrations of oscillatory bases, and the other is the controller, which dominates Cartesian trajectory tracking. The principal advantage is that the pseudo-inverse Jacobian control only need to select control gains for Cartesian position tracking; that is, one does not need to redesign a vibration damping controller for such a system.

Moreover, the closed-loop characteristic polynomial is

$$\Delta_c(s) = |s^3I + K_ds^2 + K_ps + K_i| \tag{21}$$

Selecting diagonal control gains yields

$$K_d = \mathbf{diag}\{k_{d_i}\}, \quad K_p = \mathbf{diag}\{k_{p_i}\}, \quad K_i = \mathbf{diag}\{k_{i_i}\}$$

By using the Routh test, closed-loop stability requires that

$$k_{i_i} < k_{d_i} k_{p_i} \tag{22}$$

that is, the integral gain should not be excessively large [19].

However, the principal challenge in generating a satisfactory outer-loop PID is tuning the PID controller parameters to achieve a desired performance. The approach of selecting parameters based on experimental results is typically time-consuming. The Ziegler–Nichols tuning approach is broadly accepted as an accurate heuristic scheme for determining the proper settings for PID and PI controllers for a wide range of industrial processes. However, manual tuning is not frequently employed in practice because it is laborious and time-consuming, particularly for processes with large time constants.

Moreover, [19] proposed another scheme for selecting PD gains. The standard form of the closed-loop characteristic polynomial is

$$\Delta_c(s) = |s^2 I + k_{d_i} s + k_{p_i}| = s^2 + 2\zeta\omega_n s + \omega_n^2 \tag{23}$$

where ζ is the damping ratio, and ω_n is the natural frequency. Therefore, the desired performance in each component of the error $e(t)$ may be achieved by selecting the PD gains $k_{p_i} = \omega_n^2, k_{d_i} = 2\zeta\omega_n$.

However, determining the damping ratio and natural frequency for each component in the system is difficult. Selecting the integer (I) control gain is also difficult. Thus, an efficient method for selecting the PID control gains is needed.

3. Grey relational analysis

3.1. Development of the prediction model

The remainder of this section describes the standard derivation procedure associated with the Grey model based on experimental results obtained by other studies. Grey model GM(1,1) is employed to establish a grey predictor. The GM(1,1) comprises the fundamental operations for modeling. The prediction model was developed elsewhere [9,21,23].

3.2. Grey relational grade analytical algorithm

This subsection presents the grey relational approach for analyzing system output (Cartesian tracking error) sensitivity to small perturbations in outer-loop PID controller parameters for the Cartesian computed-torque law. Grey relational analysis is employed to rank the importance of PID control gains. Grey relational analysis is described as follows. The computation technology is similar to that described elsewhere [9,21,23].

Step 1. Calculate the comparison series x_j

The Cartesian tracking error is defined by $e_H(kT) = H_d(kT) - H(kT)$, where $H_d(kT)$ the desired Cartesian trajectory, $H(kT)$ is the end-effector Cartesian position, k is an integer, and T is sampling period. Thus, the comparison series x_j can be defined as the Cartesian tracking error for the end-effector of the manipulator in a normalized root-mean-square (RMS) formulation

$$x_j = \sqrt{\sum_{k=1}^{N} e_H^2}/N, \tag{24}$$

where N is the total number of samples.

Step 2. Calculate the reference series x_i,

$$x_i^*(k) = \frac{\min[x_j^{(0)}(k)]}{x_j^{(0)}(k)}, \tag{25}$$

where $\min[x_j^{(0)}(k)]$ is the minimum values in a comparison series at the kth experimental datum.

Step 3. The absolute differences of a given series are compared via

$$\Delta_{ij}(k) = |x_i(k) - x_j(k)| \tag{26}$$

where Δ_{ij} is the absolute difference between the series x_i and x_j at the kth experimental datum. Typically, x_i and x_j are defined as reference and comparison series, respectively. The values for the original series must be normalized to the same order as variations in the order of data that characterize factors results in an inaccurate grey relational grade.

Step 4. Calculate the minimum and maximum values of each experimental datum via

$$\begin{aligned} \Delta_{\min} &= \overset{\min}{\forall j} \in \overset{\min}{i} \forall k \, |x_i(k) - x_j(k)| \\ \Delta_{\max} &= \overset{\max}{\forall j} \in \overset{\max}{i} \forall k \, |x_i(k) - x_j(k)| \end{aligned} \tag{27}$$

Step 5. Estimate the grey relational coefficient using $\gamma(x_i(k),x_j(k))$

The calculated grey relational coefficient (GRC) expresses the relationship between control performance, which is an estimated reference sequence, and its sequences that are compared. Eq. (28) yields the GRC of (x_i,x_j) at the k-th corresponding datum. The GRC can be intuitively regarded as the point-to-point relationship at the k-th corresponding datum.

$$\gamma(x_i(k), x_j(k)) = \frac{\Delta_{\min} + \zeta \Delta_{\max}}{\Delta_{ij}(k) + \zeta \Delta_{\max}} \tag{28}$$

where ζ is the distinguishing coefficient; its interval is bounded on $\zeta \in [0, 1]$ and frequently taken as 0.5. The factor ζ in Eq. (28) controls the resolution between $\Delta_{\max}$ and $\Delta_{\min}$. The operator can select a value between 0 and 1 to suit the application. Additionally, $\Delta_{\min}$ and $\Delta_{\max}$ are the minimum and maximum differences between the reference sequence and all other sequences, respectively.

Step 6. Estimate the grey relationship grade (GRG) $\Gamma(x_i, x_j)$

The grey relational grade (GRG) is employed to describe and elucidate the relationship between two sets of comparison and reference under a particular background. A large GRG between two tasks indicates that the tasks are closely related. Restated, task that are very similar have a large GRG. When estimating the effort expended by a PID controller, the GRG is the strength of the relationship between an estimated control performance (reference series) and its historical values (comparison series). The GRG is defined as the mean of the GRCs at the effort drivers. Here, $\Gamma(x_i, x_j)$ is designed as GRG between $x_i(k)$ and $x_i(k)$

$$\Gamma(x_i, x_j) = \frac{1}{n} \sum_{k=1}^{n} \gamma(x_i(k), x_j(k)) \tag{29}$$

where n is the number of effort drivers identified during the estimation procedure. In the tracking-control experiment, the GRG is associated with the impact of the PID control gains for the estimated Cartesian computed-torque law for tracking error.

4. Experimental implementation

An experimental device was designed and constructed to verify both model development and controller design. For a description of this device, see [6–9]. Fig. 3 shows the experimental apparatus. Test results are obtained via the aforementioned procedures using MATLAB and Simulink. Two servomotors are attached to each joint, and optical encoders are used to measure the position of the motor shaft. Optical encoders are used as the positional feedback device for sensing the angular displacement of the motor shaft. Furthermore, base compliance was achieved by four linear springs (stiffness of each spring is 200 N/m). To analyze the transverse oscillations of the base, a PCB PIEZOTRONICS force sensor (model 208C01) was attached to the face of the oscillatory base to measure base transverse vibrations. Moreover, a force generator is generating a damping force that suppresses vibration of oscillatory bases. The implementation of the proposed controller is indicated in Fig. 4.

5. Results and discussion

5.1. Estimation for grey relational grade Γ

Grey relational analysis is utilized to determine the sensitivity of tuning outer-loop PID parameters to attain a desired performance based on the Cartesian computed-torque control law. The simulations and experimental results are specified the desired task of the robot manipulator mounted on the oscillatory bases. Since the manual computation associated in grey analysis is tedious and prone to errors, an automated computational process is highly desirable. Therefore, a program written in Microsoft EXCEL is developed for this work. Data are input and the program then automatically derives the dynamic equations for a given system. Additionally, in this program, no ranking errors affect operations. Hence, the results of the analysis are more convincing than those obtained by manual computation.

The end-point Cartesian position X- and Y-direction vector of such a manipulator system is:

$$\begin{aligned} x_2 &= a_1 \cos\theta_1 + a_2 \cos(\theta_1 + \theta_2) \\ y_2 &= a_1 \sin\theta_1 + a_2 \sin(\theta_1 + \theta_2) + x_b. \end{aligned} \tag{30}$$

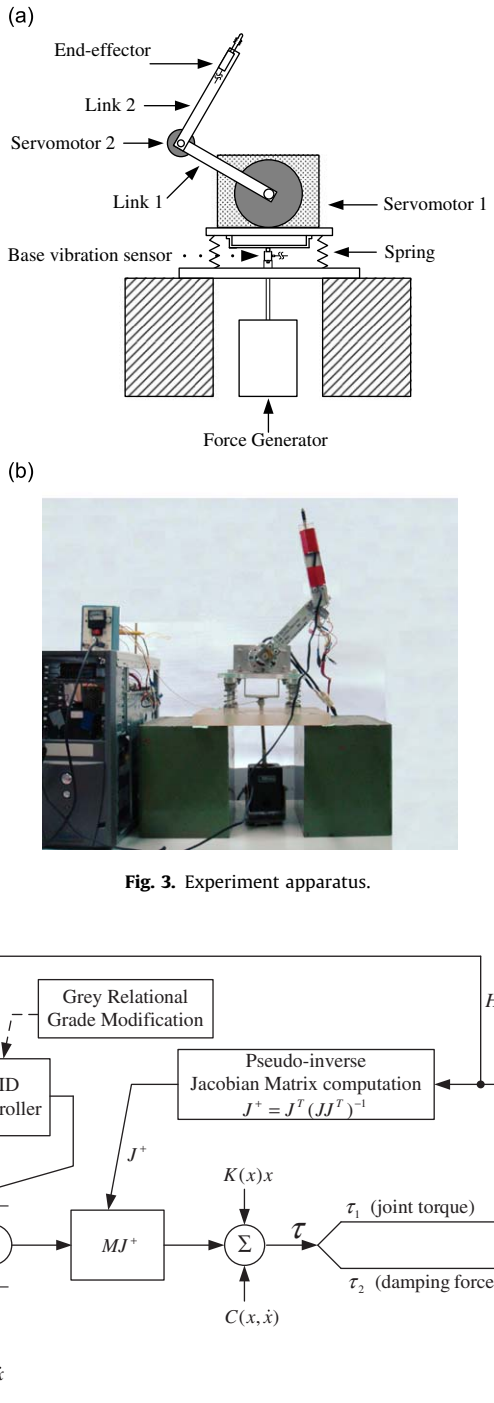

Fig. 3. Experiment apparatus.

Fig. 4. Implementation of the controller.

Therefore, Jacobian matrix J is a nonsquare matrix and a redundant robot condition occurs. Hence, the pseudo-inverse Jacobian matrix is applied for such a system. Moreover, point accuracy has been determined while accounting for base transverse vibrations. Calculation of the GRG follows the procedure presented in Section 3.2. Table 1 presents computational results yielded by Eqs. (24)–(29) for X-direction tracking. Table 1 also presents the normalized RMS tracking error, e_x, for various K_{px}, K_{ix}, and K_{dx} control gains. Table 1 also shows the GRC γ and its relational grade for X-direction tracking, Γ. The GRG Γ is 0.82725 for K_{px}, 0.85420 for K_{dx}, and 0.72134 for K_{ix}. Hence, the sensitivities of parameter perturbations are obtained easily. Furthermore, tuning K_{dx} for the PID controller is more sensitive than that for tuning K_{px}, and K_{ix} in X-direction tracking behavior (Table 1). The ranked importance of control gains is $K_{dx} > K_{px} > K_{ix}$. The

Table 1
Grey relational grade for *X*-direction.

Cartesian coordinates *X*-direction								
Design			Eq. (24) x_j	Eq. (25) x_i	Eq. (26) Δ_{ij}	Eq. (28) γ	Eq. (29) Γ	Rank
$K_{px}=10$	$K_{dx}=10$	$K_{ix}=0$	0.00756	0.56878	0.56122	1.00000	**0.82725**	2
$K_{px}=20$			0.00560	0.76786	0.76226	0.84046		
$K_{px}=30$			0.00477	0.90147	0.89670	0.75944		
$K_{px}=40$			0.00430	1.00000	0.99570	0.70910		
$K_{px}=40$	$K_{dx}=10$	$K_{ix}=0$	0.00430	1.00000	0.99570	0.70910	**0.85420**	1
	$K_{dx}=20$		0.00536	0.80224	0.79688	0.81799		
	$K_{dx}=30$		0.00638	0.67398	0.66760	0.90872		
	$K_{dx}=40$		0.00730	0.58904	0.58174	0.98099		
$K_{px}=40$	$K_{dx}=10$	$K_{ix}=10$	0.00433	1.00000	0.99567	0.70911	**0.72134**	3
		$K_{ix}=20$	0.00441	0.98186	0.97745	0.71787		
		$K_{ix}=30$	0.00448	0.96652	0.96204	0.72545		
		$K_{ix}=40$	0.00455	0.95165	0.94710	0.73295		
				Eq. (27) $\Delta_{\min}$ 0.56122	$\Delta_{\max}$ 0.99570			

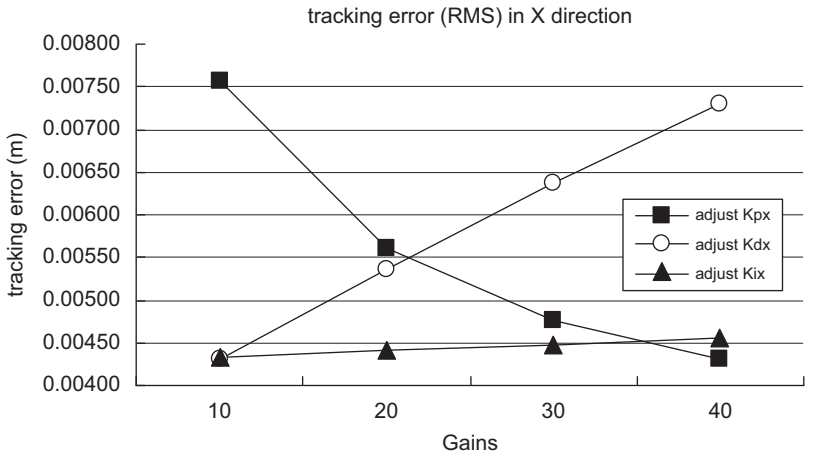

Fig. 5. Tracking error vs. control gains in *X*-direction.

priority of modifying controller parameters should be highest among parameters. Based on the GRG between tracking error and PID control gains, all control gains can be ranked according to GRG. This procedure is called grey relational ranking. Consequently, an operator can make an appropriate decision based on the grey ranking and the control goal can be attained. An existing GRG close to unity corresponds to a strong similarity among geometric patterns that characterize any two series. Notably, as K_{px} gain increases, tracking error decreases (Fig. 5). Conversely, Fig. 5 also indicates that as K_{dx} (or K_{ix}) gain increases, tracking error increases. Therefore, one can follow the above rules when adjusting PID control gains to determine whether to increase (or decrease) the control gains.

Table 2 shows the GRC γ and its relational grade Γ for *Y*-direction tracking. Fig. 6 shows tracking error vs. control gains in the *Y*-direction. The results are similar to those for *X*-direction tracking. The ranked importance of control gains is $K_{dy} > K_{py} > K_{iy}$. Thus, reduced tracking error is maximal when parameter K_{dy} is tuned, indicating that parameter K_{dy} is the most important parameter when tuning the controller. The proposed grey relational analysis methodology can be employed to rank parameter importance. The most important parameter typically dominates in base control; the next most important parameters are used to modify the fine motion. Hence, control parameters with the highest priorities should be modified first. Thus, the proposed grey relational analysis offers several implementation benefits—it is simple, low-cost, requires minimal computational time, and has a fast adaptation rate during implementation. A number of experiments were performed using the PID grey model to assess the merits of concepts.

Table 2
Grey relational grade for *Y*-direction.

Cartesian coordinates *Y*-direction								
Design			Eq. (24) x_j	Eq. (25) x_i	Eq. (26) Δ_{ij}	Eq. (28) γ	Eq. (29) Γ	Rank
$K_{py}=10$	$K_{dy}=10$	$K_{iy}=0$	0.01707	0.57030	0.55323	1.00000	**0.82483**	2
$K_{py}=20$			0.01265	0.76939	0.75674	0.83743		
$K_{py}=30$			0.01079	0.90214	0.89135	0.75613		
$K_{py}=40$			0.00973	1.00000	0.99027	0.70578		
$K_{py}=40$	$K_{dy}=10$	$K_{iy}=0$	0.00973	1.00000	0.99027	0.70578	**0.85188**	1
	$K_{dy}=20$		0.01211	0.80387	0.79177	0.81464		
	$K_{dy}=30$		0.01442	0.67503	0.66062	0.90708		
	$K_{dy}=40$		0.01647	0.59108	0.57461	0.98001		
$K_{py}=40$	$K_{dy}=10$	$K_{iy}=10$	0.00982	1.00000	0.99018	0.70582	**0.71803**	3
		$K_{iy}=20$	0.00999	0.98260	0.97261	0.71427		
		$K_{iy}=30$	0.01016	0.96665	0.95649	0.72220		
		$K_{iy}=40$	0.01032	0.95165	0.94133	0.72982		
				Eq. (27)				
				$\Delta_{\min}$	$\Delta_{\max}$			
				0.55323	0.99027			

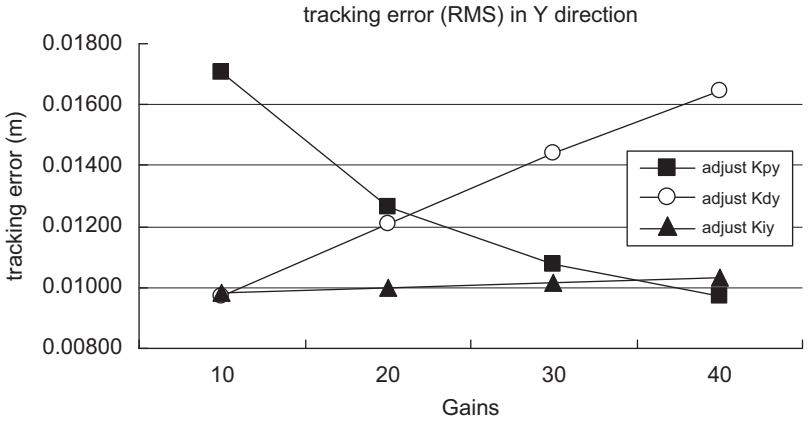

Fig. 6. Tracking error vs. control gains in *Y*-direction.

5.2. Simulation results

As noted in Section 2, the pseudo-inverse Jacobian control only needs to select control gains for Cartesian position tracking. Redesigning a vibration-damping controller for such a system is unnecessary. Therefore, to confirm further controller performance, the step reference command for *X*- and *Y*-directions were applied to the system. According to the grey relational degree described in Section 5.1, parameter K_{dx} is adjusted first to yield the best performance for *X*-direction reference inputs.

Parameters K_{px} and K_{ix} are then adjusted to acquire the best performance for reference inputs for the remaining operational range. Once these parameters are tuned, the *Y*-direction is tuned. After arbitrarily assigning values to the PID parameters [($K_{px}=50$, $K_{dx}=60$, $K_{ix}=70$),($K_{py}=50$, $K_{dy}=60$, $K_{iy}=70$)], the modification should follow the modification process (Fig. 7). First, the adjusted sequence for control parameters in the *X*-direction is

$$(K_{px}=50,K_{dx}=60,K_{ix}=70)\rightarrow(K_{px}=50,K_{dx}=15,K_{ix}=70)\rightarrow(K_{px}=65,K_{dx}=15,K_{ix}=70)$$
$$\rightarrow(K_{px}=65,K_{dx}=15,K_{ix}=0.1)$$

Performance improved significantly after the above modification methodology was applied to control parameters (Fig. 8(a)). Tracking performance was significantly improved by tuning control parameter K_{dx}. The steady-state error of the positional response was decreased markedly by the control action, indicating that parameter K_{dx} in the controller is the most important and dominates base control action. However, the improved performance achieved by tuning only parameter K_{dx} is insignificant and settling time (2.2 s) remains large. Therefore, tuning K_{px} and then K_{ix} can significantly

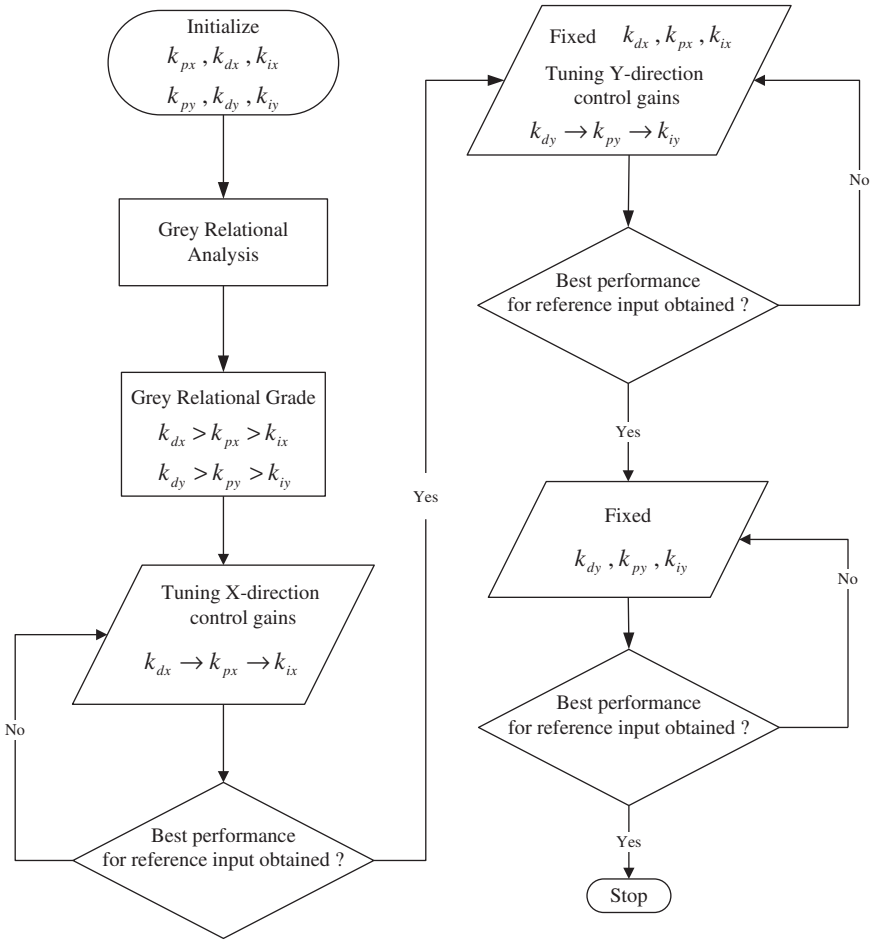

Fig. 7. Flowchart of the parameter modification process.

improve system tracking performance. After tuning parameter K_{ix}, the convergence rate accelerated (settling time was 0.8 s) and steady-state error was reduced. Consequently, the proposed modification scheme increased the convergence rate and reduced steady-state error.

When the *X*-direction tracking performance is satisfactory ($K_{px} = 65$, $K_{dx} = 15$, $K_{ix} = 0.1$), then *Y*-direction control parameters are adjusted. Similarly, the concept used to modify *Y*-direction tracking control parameters is the same as used for the *X*-direction parameters. The adjustment sequence is

$$(K_{py} = 50, K_{dy} = 60, K_{iy} = 70) \rightarrow (K_{py} = 50, K_{dy} = 20, K_{iy} = 70) \rightarrow (K_{py} = 100, K_{dy} = 20, K_{iy} = 70) \rightarrow (K_{py} = 100, K_{dy} = 20, K_{iy} = 0.2)$$

Fig. 8(b) displays the tracking performance in the *Y*-direction for various control gains. Fig. 8(c) shows that the tip position of the manipulator can move to the desired position smoothly after the proposed modification scheme was introduced.

The linear quadratic regulator (LQR) is another well-known approach for optimizing the control gains of a linear system. However, the LQR is impractical when a system has various complexities, such as nonlinearities and coupling. When system parameters are not fully known and exhibit nonlinear characteristics, selecting the weighting matrix and setting control gain *K* are very difficult tasks [18].

The Ziegler–Nichols tuning formula is a famous PID tuning scheme. The Ziegler–Nichols tuning formula is based on empirical knowledge of the ultimate gain k_u and ultimate period t_u. The PID controller is typically implemented as follows [20];

$$u = k_c\left(e + \frac{1}{T_i}\int e\mathrm{d}t - T_d\frac{\mathrm{d}y_f}{\mathrm{d}t}\right) \tag{31}$$

where the proportional gain $k_c = 0.6k_u$, the integral time $T_i = 0.5t_u$ and the derivative time $T_d = 0.125t_u$. The tracking error is defined as $e = y_d - y$, and $y_f = (1/(1 + sT_d/N))y$, where *N* is noise filtering constant.

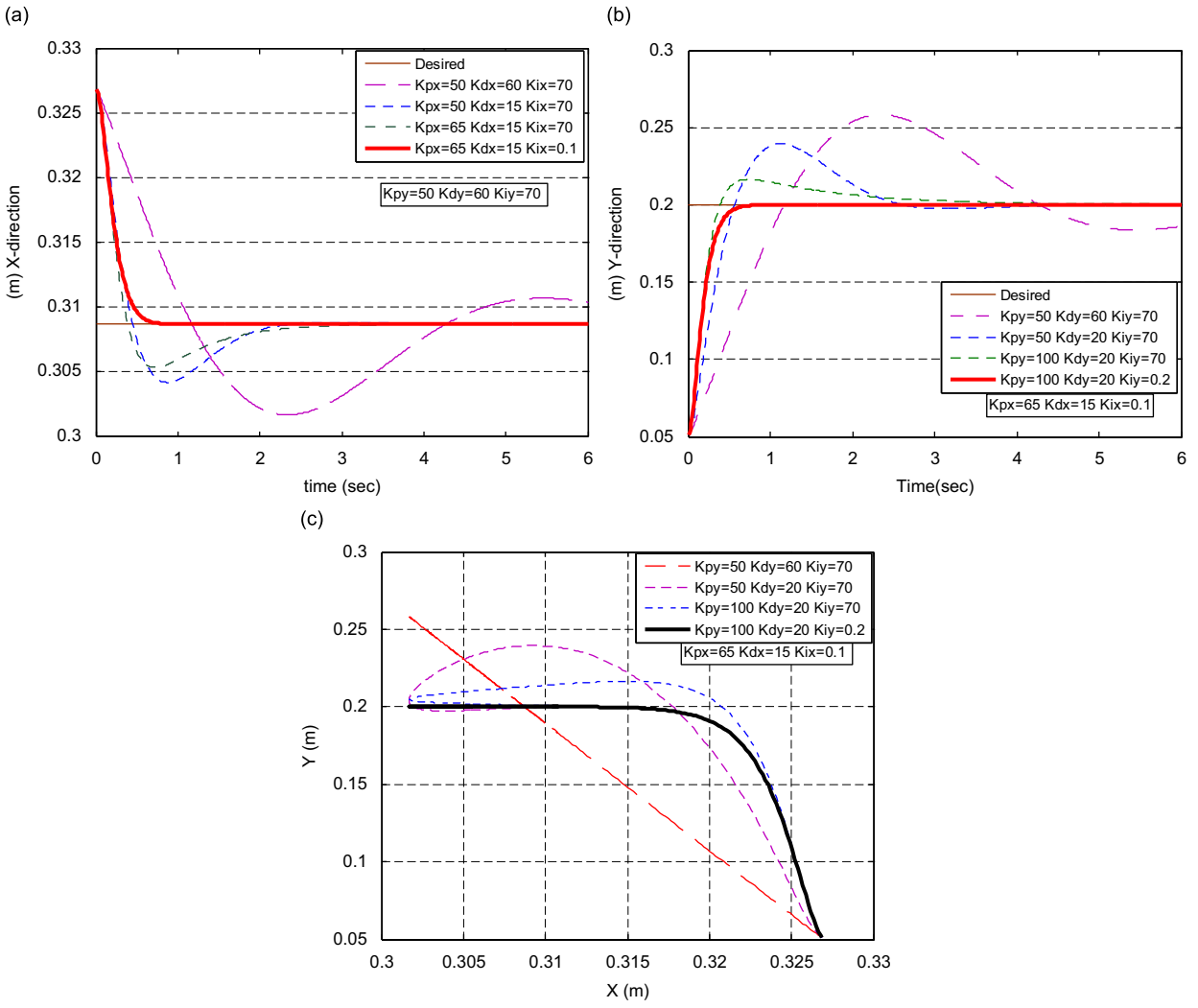

Fig. 8. Simulation results for tracking performance vs. PID control gains: (a) simulation results for tracking performance vs. PID control gains in *X*-direction; (b) simulation results for tracking performance vs. PID control gains in *Y*-direction; (c) simulation results of the tip position vs. PID control gains.

Compare to the grey PID control, the Ziegler–Nichols tuning formula needs two more values k_u and t_u to be determined. The main point of Ziegler Nichols is that it is empirical. Measure the reaction time and then derive the PID settings. However, this manual tuning scheme is not applied in practice as it is laborious and time-consuming, particularly when the time constant is large. In control process, determining ultimate gain k_u and ultimate period t_u is very difficult.

Fig. 9 presents the simulation results for the traditional Ziegler–Nichols tuning formula and the proposed grey PID methodology. According to Ziegler–Nichols tuning formula, the ultimate gain k_u and ultimate period t_u is selected as 3.43 and 2.88, respectively. The effectiveness of Cartesian tracking performance was confirmed when the proposed grey PID tuning scheme was applied. The settling time and steady-state error of the tracking response was reducibly by the grey PID control gains. However, the accuracy of the Zigler–Nichols tuning formula has been found to be quite adequate for manual tuning, as it can be supplemented by fine-tuning based on experience. It needs manual fine-tuning and human expertise to select PID control gains while in system operation. Therefore, the automation of the controller-tuning procedure, exploring the possibility of modifying the tuning formula by incorporating heuristic knowledge to replace manual fine-tuning is strong desired.

Hence, this study developed a novel fast adaptation scheme based on the GRG to select outer-loop PID control parameters for Cartesian computed-torque control. Relational analysis was used to rank easily the importance of PID control gains. The most important parameters must be identified to ensure the parameters sensitivity. The proposed grey relational methodology allows operators to adjust easily control gains while a system is operating.

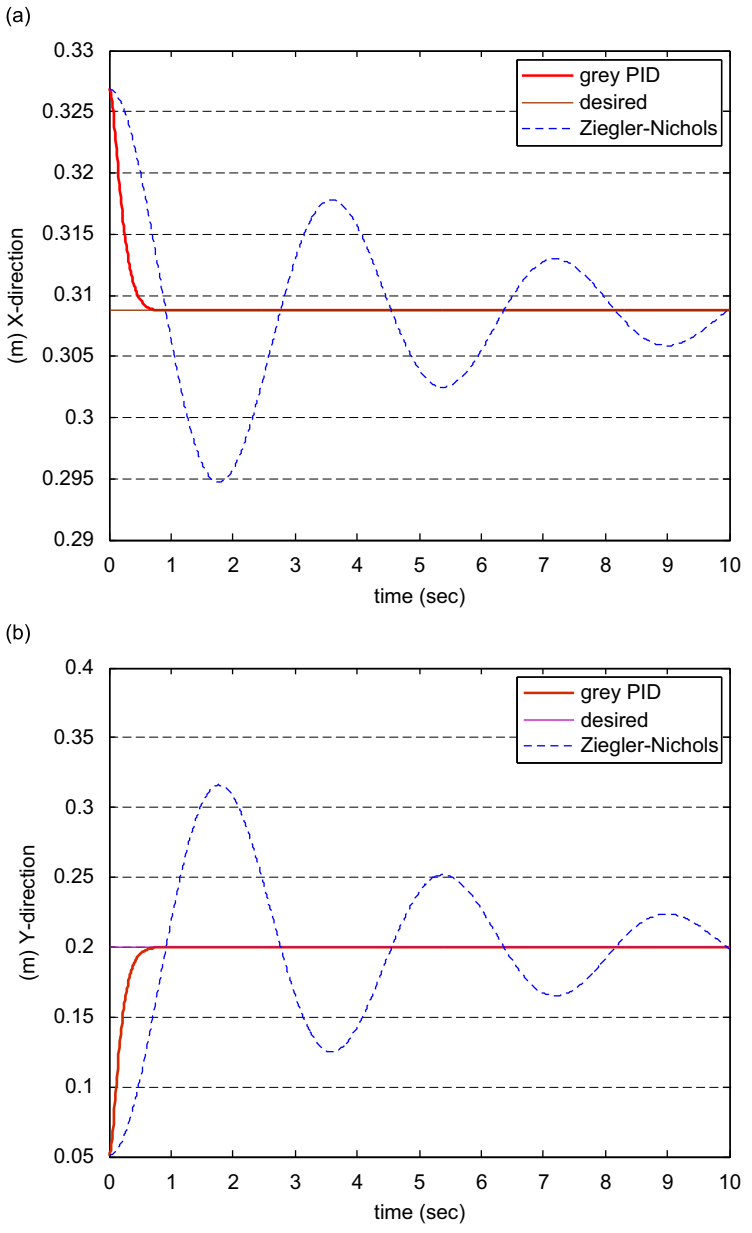

Fig. 9. Simulation results for tracking performance vs. control scheme: .(a) simulation results for tracking performance vs. control scheme in *X*-direction; (b) simulation results for tracking performance vs. control scheme in *Y*-direction.

5.3. *Experimental results*

Numerous real-time experiments were performed using the grey model of PID to assess the merits of grey relational analysis.

After arbitrarily assigning values to PID parameters, the modification should follow the grey relational process (Fig. 7). First, the adjustment sequence for control parameters is

$$(K_{px}=50, K_{dx}=40, K_{ix}=30) \rightarrow (K_{px}=50, K_{dx}=1, K_{ix}=30) \rightarrow (K_{px}=100, K_{dx}=1, K_{ix}=30)$$
$$(K_{px}=100, K_{dx}=1, K_{ix}=4)$$

Therefore, experimental results also support the same conclusion as that for position tracking response (Fig. 10a). Similarly, when *X*-direction trajectory tracking performance is satisfactory ($K_{px}=100$, $K_{dx}=1$, $K_{ix}=4$), *Y*-direction control parameters are adjusted. A substantial improvement was attained during tracking tasks when the proposed parameter

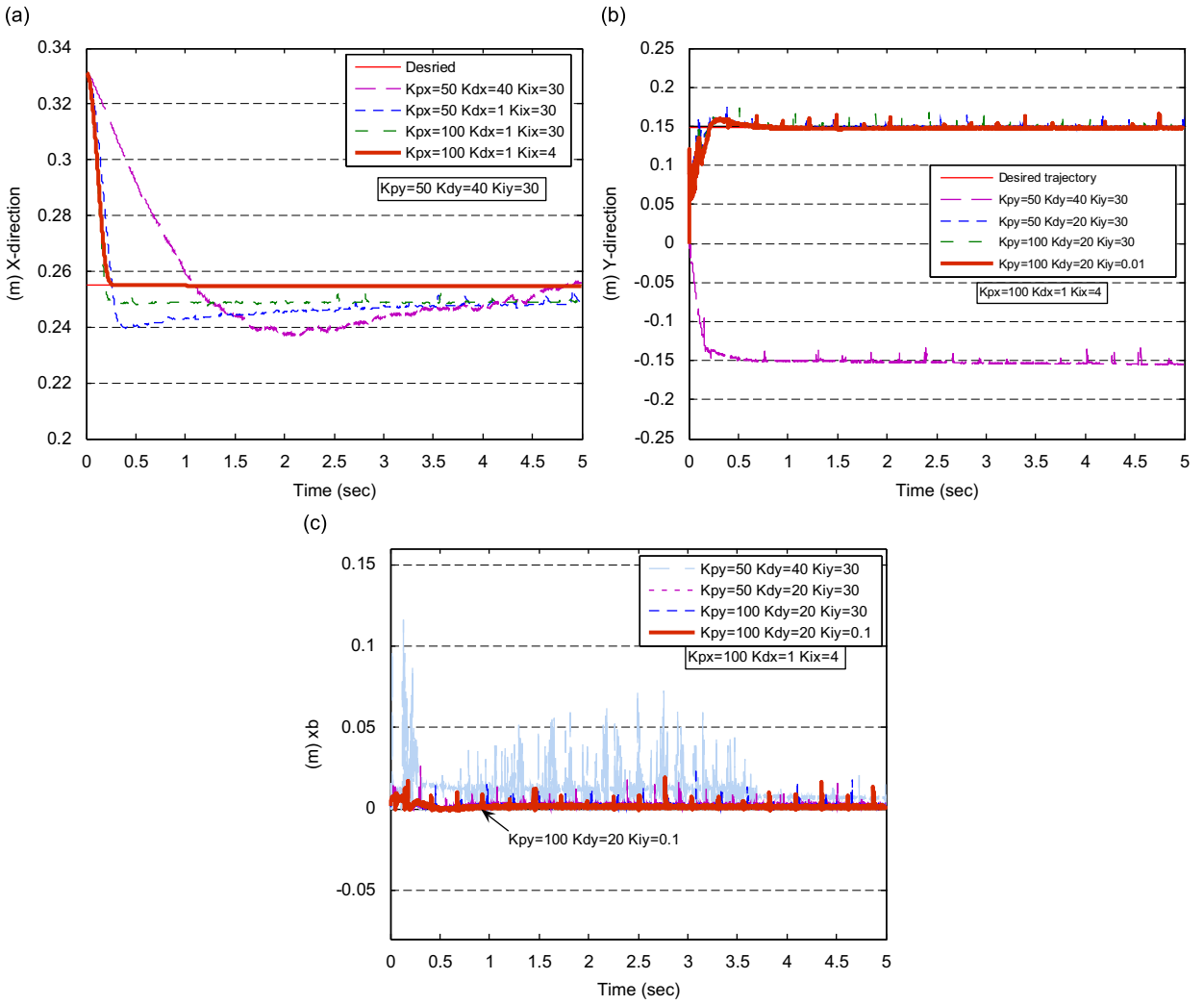

Fig. 10. Experimental results for tracking error vs. PID control gains: .(a) experimental results for tracking error vs. PID control gains in *X*-direction; (b) experimental results for tracking error vs. PID control gains in *Y*-direction; (c) experimental results of the oscillatory base vibration displacement vs. PID control gains.

modification scheme was adopted (Fig. 10b). The settling and steady-state error of the end-effector position response was reduced markedly by the control action. We conclude that the controller was effective in tuning grey PID parameters (Fig. 10). These experimental results indicate that good tracking performance can be achieved (Figs. 10a and b) and base oscillation eliminated (Fig. 10c). Consequently, the proposed scheme improves Cartesian endpoint accuracy. Even when a controller only selects control gains for Cartesian position tracking, base oscillation can be decreased. Such gain control should reduce the effect of subsystem coupling motion on the entire system. Additionally, control gains can be tuned for a robot mounted on an oscillatory base without need for elaborate modeling and analyses.

Similarly, the experimental results also the effectiveness of the proposed grey PID scheme for tracking performance (Figs. 11a and b) and minimizing base oscillatory vibration in time domain (Fig. 11c). The grey PID control action significantly reduces the steady-state error in settling time, demonstrating that the convergence rate is faster than Ziegler–Nichols tuning scheme.

5.4. Test results with model uncertainties

In addition, this study also investigates the control of the robot manipulators mounted on oscillatory bases when their dynamical model is uncertain. Simulations like those presented in this subsection could be carried out for approximate Cartesian computed-torque control which demonstrated in Eq. (20). The basic principles for the tuning grey PID control

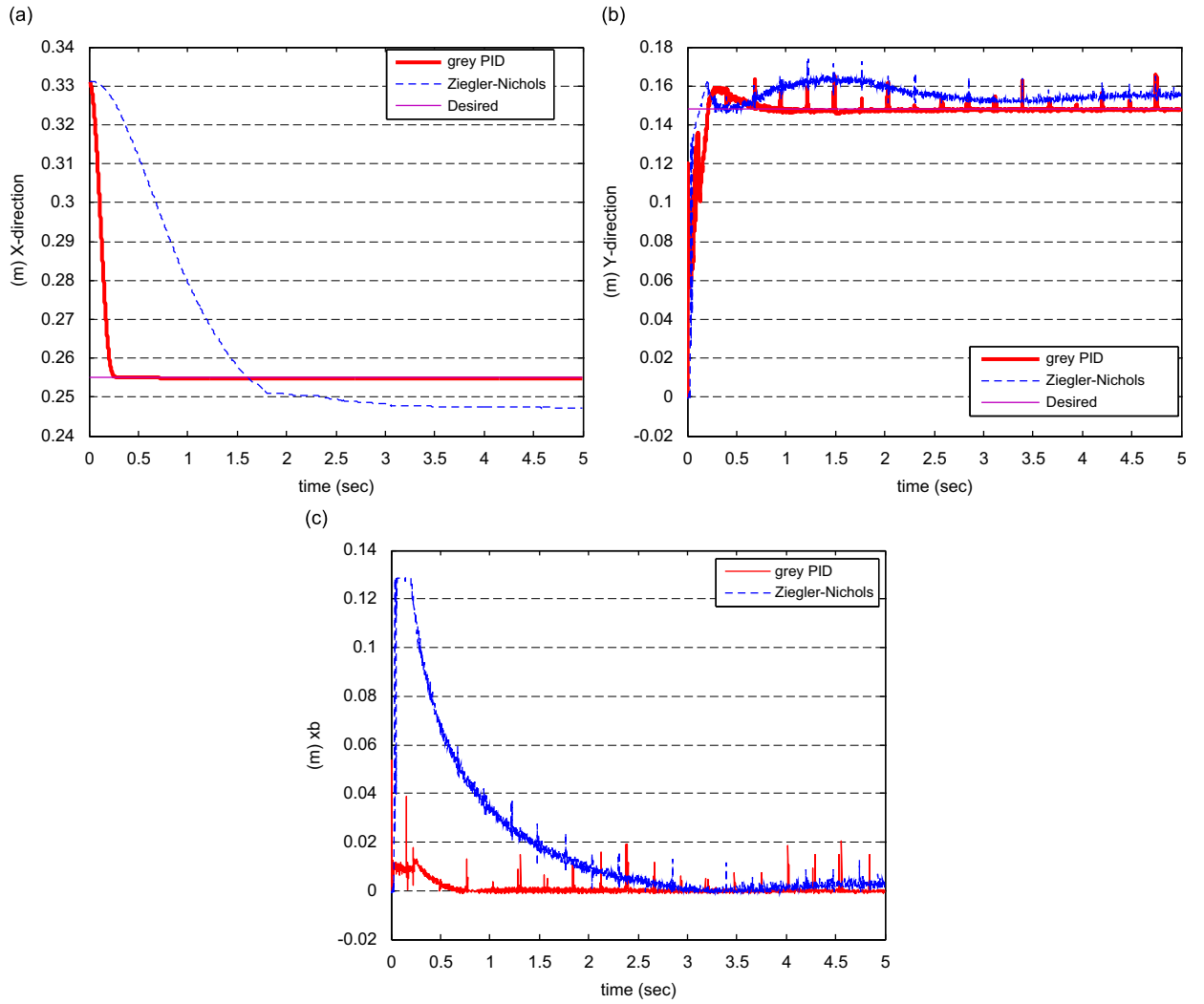

Fig. 11. Experimental results for tracking performance vs. control scheme: (a) experimental results for tracking performance vs. control scheme in *X*-direction; (b) experimental results for tracking performance vs. control scheme in *Y*-direction; (c) experimental results of the oscillatory base vibration displacement vs. control scheme.

gains would be the same as for the Cartesian computed-torque control while the model is assume exactly known. The PID parameters modification also follows the adaptation process (Fig. 7). Tracking performance was significantly improved by tuning control gains K_{dx} and K_{dy}. The steady-state error of the positional response was decreased markedly by the control action, indicating that parameter K_{dx} and K_{dy} in the controller is the most important and dominates base control action for *X*- and *Y*-direction, respectively. Hence, simulation results support the same conclusion as that for position tracking response (Fig. 12a and b). Fig. 12(c) shows that the end-effector of the manipulator can move to the desired Cartesian position smoothly after the proposed modification scheme was introduced. Therefore, even if the dynamic systems are not known exactly, the performance of controllers based on Eq. (20) can be quite good if the outer-loop gains are selected appropriately. In less demanding applications, or when the dynamic model of the process is poorly known, PID control may still be used [19,20].

Furthermore, Fig. 13 indicates that the experimental results for tracking performance in using grey PID scheme with approximate Cartesian computed-torque control law. The experimental results also demonstrate the successfully tracking performance when the dynamical model is uncertain (Fig. 13). The tip position of the manipulator can move to the desired Cartesian position efficiently after the proposed grey modification method was applied. Thus, even if the dynamic model is inadequately known, the proposed grey relational methodology as well allows the operators to adjust easily control gains while a system is operating. Consequently, the robustness properties of pseudo-inverse Jacobian control with grey relational analysis make a successful control law for many applications.

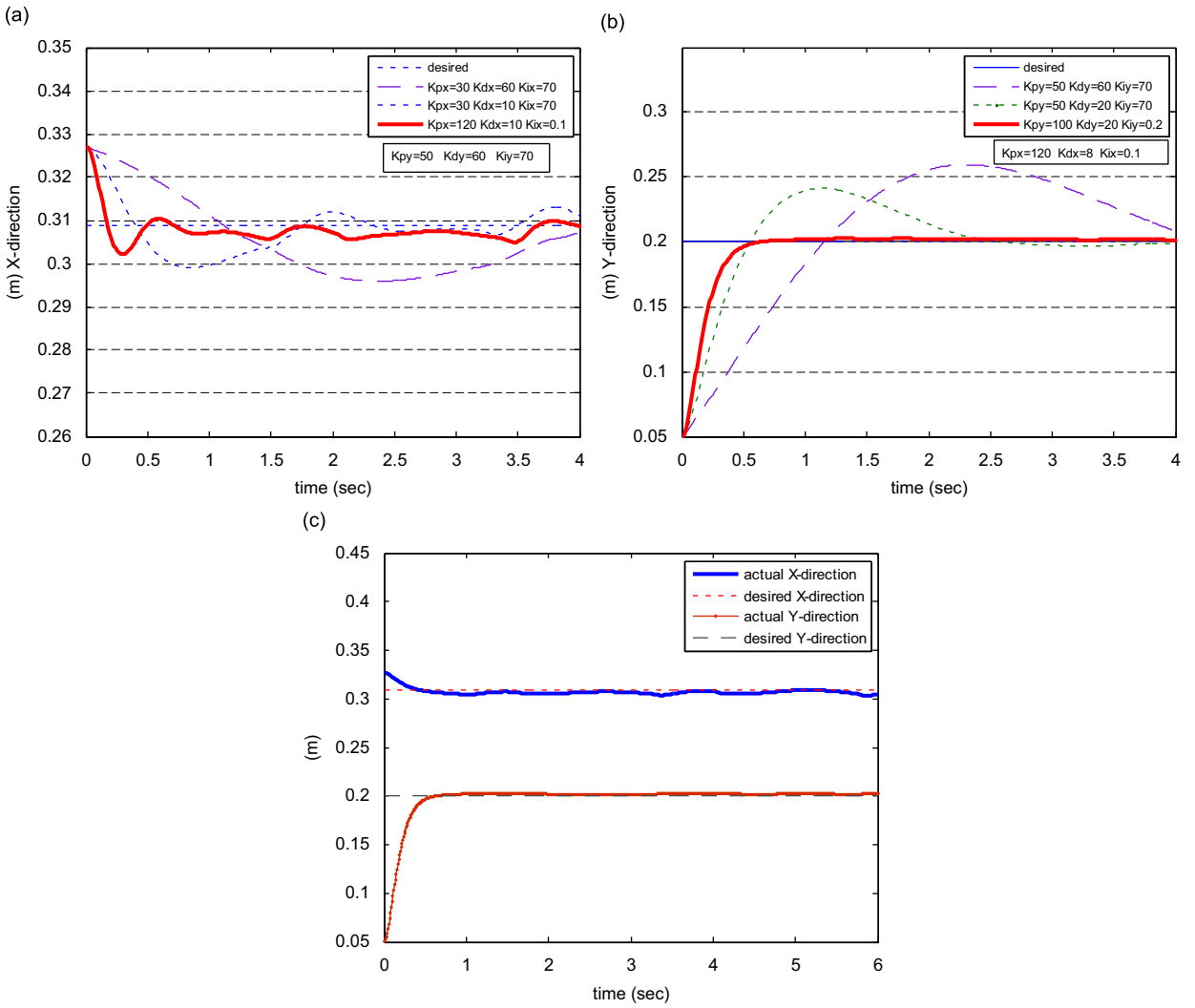

Fig. 12. Simulation results for tracking performance vs. control scheme (ACCTC):.(a) simulation results for tracking performance vs. PID control gains in *X*-direction (ACCTC); (b) simulation results for tracking performance vs. PID control gains in *Y*-direction (ACCTC); (c) simulation results for tracking performance by grey PID scheme with ACCTC.

6. Conclusions

The pseudo-inverse Jacobian feedback control laws with grey relational analysis for tuning outer-loop PID control parameters of Cartesian computed-toque control law was successfully applied for robot manipulators mounted on oscillatory bases. From the projection operator, the whole system can be divided into two control loops—one is the damping controller that suppresses vibrations of oscillatory bases, and the other is the controller, which dominates Cartesian trajectory tracking. The primary advantage is that the proposed pseudo-inverse Jacobian control only need to select control gains for Cartesian position tracking; that is, one does not need to redesign a vibration damping controller for such a system. Grey relational grade is utilized to investigate the sensitivity of tuning the auxiliary signal PID of the Cartesian computed-torque law to achieve desired performance. It indicates that the ranking importance is $K_d > K_p > K_i$ for *X*- and *Y*-directions tracking control, respectively. The priority modification of the controller parameters should be the top ranking importance among the parameters. The test results of position response have shown that the tracking performance can be achieved and base oscillation eliminated. The results of this study can be feasible to various mechanical systems, such as mobile robot, gantry cranes, underwater robot, and other dynamic systems mounted on oscillatory bases for moving the end-effector to a desired Cartesian position. However, the control of the robot end-effector to a desired Cartesian position is the preliminary study of the hybrid position/force control. Therefore, the future work will be focus on the issue of hybrid force/position control of the robots with oscillatory base interacting with geometrically unknown environments.

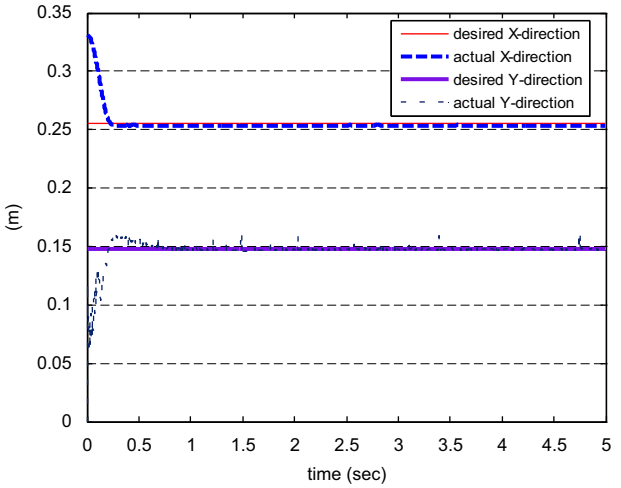

Fig. 13. Experimental results for tracking performance by grey PID scheme with ACCTC.

Acknowledgements

The authors would like to thank the National Science Council of the Republic of China, Taiwan for financially supporting this research under Contract No. NSC 95-2221-E-231-010-.

References

[1] J.Y. Lew, S.-M. Moon, Acceleration feedback control of compliant base manipulators, *Proceedings of 1999 American Control Conference*, San Diego, CA, 1999, pp. 1955–1959.
[2] J.Y. Lew, S.-M. Moon, A simple active damping control for compliant base manipulators, *IEEE/ASME Transactions on Mechatronics* 6 (3) (2001) 305–310.
[3] M. Toda, An H_∞ control-based approach to robust control of mechanical systems with oscillatory bases, *IEEE Transactions on Robotics and Automation* 20 (2) (2004) 283–296.
[4] M.W. Spong, Modeling and control of elastic joints, *ASME Journal of Dynamic Systems, Measurement, and Control* 109 (1987) 310–319.
[5] K. Osuka, F. Matsuno, On robustness of passivity of manipulators, *Proceedings of IEEE Conference on Decision and Control*, 1999, pp. 3406–3409.
[6] J. Lin, Multi-timescale fuzzy controller for a continuum with a moving oscillator, *IEE Proceedings—Control Theory and Applications* 151 (3) (2004) 310–318.
[7] J. Lin, Z.Z. Huang, A hierarchical fuzzy approach to supervisory control of robot manipulators with oscillatory bases, *IFAC Mechatronics* 17 (10) (2007) 589–600.
[8] J. Lin, Z.Z. Huang, P.H. Hsiao, An active damping control of robot manipulators with oscillatory bases by singular perturbation, *Journal of Sound and Vibration* 304 (1–2) (2007) 345–360.
[9] J. Lin, Z.-Z. Huang, A novel PID control parameters tuning approach for robot manipulators mounted on oscillatory bases, *Robotica* 25 (4) (2007) 467–477.
[10] L.E. George, W.J. Book, Inertial vibration damping control of a flexible base manipulator, *IEEE/ASME Transactions on Mechatronics* 8 (2) (2003) 268–271.
[11] M. Takegaki, S. Arimoto, A new feedback method for dynamic control of manipulators, *Transactions of the ASME, Journal of Dynamic Systems, Measurement, and Control* 103 (2) (1981) 119–125.
[12] S. Arimoto, *Control Theory of Nonlinear Mechanical Systems: A Passivity-based and Circuit-theoretic Approach*, Oxford University Press, Oxford, UK, 1996.
[13] S. Arimoto, H. Hashiguchi, M. Sekimoto, R. Ozawa, Generation of natural motions for redundant multi-joint systems: a differential-geometric approach based upon the principle of least actions, *Journal of Robotic Systems* 22 (11) (2005) 583–605.
[14] M. Sekimoto, S. Arimoto, A natural redundancy-resolution for 3-D multi-joint reaching under the gravity effect, *Journal of Robotic Systems* 22 (11) (2005) 607–623.
[15] S. Chiaverini, G. Oriolo, I.D. Walker, Kinematically redundant manipulators, in: B. Sicilliano, O. Khatib (Eds.), *Springer Handbook of Robotics*, Springer-Verlag, New York, 2008, pp. 245–268.
[16] C.C. Cheah, M. Hirano, S. Kawamura, S. Arimoto, Approximate Jacobian control for robots with uncertain kinematics and dynamics, *IEEE Transactions on Robotics and Automation* 19 (4) (2003) 692–702.
[17] L.-A. Dessaint, S. Robert, M. Saad, G. Olivier, A Cartesian-based adaptive tracking controller for SCARA robot, *Proceedings of the International Conference on IECON '93 Industrial Electronics, Control, and Instrumentation*, 1993, pp. 1517–1521.
[18] J.Y. Lew, Contact control of flexible micro-macro-manipulators, *Proceedings of the 1997 IEEE International Conference on Robotics and Automation*, Albuquerque, New Mexico, April 1997, pp. 2850–2855.
[19] F.L. Lewis, C.T. Abdallab, D.M. Dawson, *Control of Robot Manipulators*, Macmillan, London, 1994.
[20] C.C. Hang, K.J. Åström, W.K. Ho, Refinements of the Ziegler–Nichols tuning formula, *IEE Proceedings—D* 138 (2) (1991) 111–118.
[21] J. Deng, Introduction to grey system theory, *The Journal of Grey System* 1 (1989) 1–24.
[22] P. Chiachio, Y. Bouffard-Vercelli, F. Pierrot, Force polytope and force ellipsoid for redundant manipulators, *Journal of Robotic Systems* 14 (8) (1997) 613–620.
[23] J. Lin, H. Chiang, C.C. Lin, Tuning PID control gains for micro Piezo-stage in using grey relational analysis, *International Conference on Machine Learning and Cybernetics*, July 12–15, 2008, pp. 3863–3868.